

spherule bed was originally composed of impact-glass spherules ejected from the putative KT impact crater on the Yucatan peninsula. The impact nature of the spherule bed was confirmed by the previous identification of shocked quartz and relict impact glass. These melt-glass spherules were deposited on a shallow shelf, probably located north-northwest of the present sites in the Mendez basin [3]. Thick, unstable deposits of these spherules were mobilized as debris flows at the mouths of canyons in the shelf/slope by either tsunamis, earthquakes, or storms (associated with the KT impact).

The debris flows either generated their own turbidity currents involving unconsolidated shelf sands, as has been calculated theoretically and observed experimentally [6], or these sands were mobilized into turbulent flow simultaneously with the spherules, unmixing from the latter by a sieve mechanism operating on relative particle sizes and flow densities. An alternative to this single-pulse hypothesis is that of two separate episodes, wherein the spherule-laden debris flows were separate events that preceded the turbidity-flow units slightly in time. Arguing against the latter dual-pulse hypothesis is the lack of significant amounts of spherule-bearing material incorporated in the base of the sandstone unit, which should occur if this unit originated later as a separate turbidity flow that scoured the top of the previously deposited debris flow.

Either process resulted in debris flows consisting of glass spherules that scoured and filled shallow channels in basinal Mendez marls, followed closely by sand in turbid suspension that was deposited on top of the spherule beds in the neoformed channels. This model resembles the modern example of upper Pleistocene chaotic silt beds transported by debris flows (analogous to the spherule beds) and directly overlain by turbidite sand beds in distal, channelized, outer-fan lobes of the Mississippi delta in the Gulf of Mexico [7]. As in this example, the presence of relatively undeformed clasts in the Mexican spherule beds suggests deposition in a non-turbulent, debris-flow regime.

Channel scouring by the debris flow is exemplified by the rip-up clasts of underlying Mendez marl contained in this bed. Also, the bed is deposited in a typical shallow-channel profile with clearly defined edges. Both the spherule unit and the sandstone unit contain benthic foraminifers of late Maastrichtian age from a shallow neritic environment, whereas benthic taxa are rare in the underlying, deep-water, Mendez marl [3,8]. This strongly suggests that these clastic units are allochthonous, having been transported from shallow water to their present basinal setting.

The sandstone unit at Mimbral displays sedimentary features similar to those that define a turbidite. For comparison, these features have been defined as divisions of the Mimbral sandstone unit in Fig. 1a, using the same nomenclature ( $T_{a-c}$ ) that subdivides a classic turbidite sequence (Fig. 1b).

The final, fine-grained phase of turbidite deposition and commencement of the hemipelagic rain coincided with the arrival of the last portion of the fireball layer at the seafloor; components identifying this partial fireball layer are an Ir anomaly and magnetite spinel crystals [9]. The presence of a capping fireball layer limits the time of formation of this clastic unit to a period of up to several months following impact, according to our single-impact KT model [9].

The almost instantaneous loading of a thick deposit of glass spherules (up to 3 mm in diameter) onto a shallow shelf constitutes a rather rare event that may, when mobilized, produce unique

deposits. For the reasons stated above, we interpret the clastic sequences at Mimbral and La Lajilla as spherule-bearing, debris-flow units overlain by sandstone turbidite units. Furthermore, both of these clastic units were mobilized on a distant shelf/slope soon after impact by the effects of seismic or oceanic disturbances associated with the KT impact event.

**References:** [1] Alvarez W. et al. (1992) *GSA Abstr.*, 24, 7, A331. [2] Smit J. et al. (1992) *Geology*, 20, 99–103. [3] Stinnesbeck W. et al. (1993) *Geology*, 21, 797–800. [4] Bohor B. F. et al. (1993) *LPS XXIV*, 145–146. [5] Bohor B. F. and Betterton W. J. (1993) *LPS XXIV*, 143–144. [6] Hampton M. A. (1972) *J. Sed. Petrol.*, 42, 775–793. [7] Nelson C. H. et al. (1992) *Geology*, 20, 693–696. [8] Keller G. et al. (1992) *GSA Abstr.*, 24, A332. [9] Pollastro R. M. and Bohor B. F. (1993) *Clays, Clay Minerals*, 41, 7–25. [10] Howell D. G. and Normark W. R. (1982) in *Sandstone Depositional Environments* (P. Scholle and D. Spearing, eds.), AAPG, 365–404.

**N94-28296**

5 208812 P-3  
**AXIAL FOCUSING OF IMPACT ENERGY IN THE EARTH'S INTERIOR: PROOF-OF-PRINCIPLE TESTS OF A NEW HYPOTHESIS.** M. B. Boslough, E. P. Chael, T. G. Trucano, M. E. Kipp, and D. A. Crawford, Sandia National Laboratories, Albuquerque NM 87185, USA.

Along with the appreciation of the importance of impact events on the Earth's evolution, there has been increasing speculation that energetic collisions have been responsible for processes as varied as continental flood basalt eruptions, mantle plumes, continental rifting, and geomagnetic pole reversals. The link between impacts and such geophysical processes was first discussed by Seyfert and Sirkin [1], who suggested that impact-induced mantle plumes could be a mechanism for initiating the breakup of plates. Burek and Wänke [2] listed correlations between known Cenozoic impacts and geomagnetic field reversals, unconformity ages, shifts in paleotemperatures, and tectonic episodes. They suggested that major impacts could generate shock-induced phase transitions in the upper mantle, disrupting a delicately balanced stability down to the core-mantle boundary. Rampino and Strothers [3] proposed a quasiperiodic correlation between mass extinctions and major continental flood basalt volcanism over the last 250 m.y. and attempted to explain it in terms of episodic showers of impacting comets. Connections between impacts and the internal workings of the Earth are supported by correlations of the ages of tektites from strewn fields with geomagnetic field reversals [4], and by a reversal associated with sediments deposited immediately after the impact that formed the Ries Crater [5].

A causal link between major impact events and global processes would probably require a significant change in the thermal state of the Earth's interior, presumably brought about by coupling of impact energy. One possible mechanism for such energy coupling from the surface to the deep interior would be through focusing due to axial symmetry. Antipodal focusing of surface and body waves from earthquakes is a well-known phenomenon [6], which has previously been exploited by seismologists in studies of the Earth's deep interior [7,8]. Antipodal focusing from impacts on the Moon, Mercury, and icy satellites has also been invoked by planetary scientists to explain unusual surface features opposite some of the large impact structures on these bodies [9,10]. For example, "disrupted" terrains have been observed antipodal to the Caloris impact basin on

Mercury and Imbrium Basin on the Moon. Very recently there have been speculations that antipodal focusing of impact energy within the mantle may lead to flood basalt and hotspot activity [11,12], but there has not yet been an attempt at a rigorous model.

We have proposed a new hypothesis and performed preliminary proof-of-principle tests for the coupling of energy from major impacts to the mantle by axial focusing of seismic waves. Because of the axial symmetry of the explosive source, the phases and amplitudes are dependent only on ray parameter (or takeoff angle) and are independent of azimuthal angle. For a symmetric and homogeneous Earth, all the seismic energy radiated by the impact at a given takeoff angle will be refocused (minus attenuation) on the axis of symmetry, regardless of the number of reflections and refractions it has experienced. Mantle material near the axis of symmetry will experience more strain cycles with much greater amplitude than elsewhere and will therefore experience more irreversible heating. The situation is very different than for a giant earthquake, which in addition to having less energy, has an asymmetric focal mechanism and a larger area. It should be noted that our hypothesis is fundamentally different than those proposed by many others [e.g., 13–16], which involve melting and excavation at the impact location. Problems with models of this type have been pointed out by Loper [17].

We are using two independent proof-of-principle approaches. The first makes use of seismic simulations, which are being performed with a realistic Earth model to determine the degree of focusing along the axis and to estimate the volume of material, if any, that experiences significant irreversible heating. The second involves two-dimensional hydrodynamic code simulations to determine the stress history, internal energy, and temperature rise as a function of radius along the axis.

For the preliminary seismic modeling the impact was represented as a vertical point force applied at the Earth's surface as a delta function in time. The impactor was assumed to yield an impulse of approximately  $3 \times 10^{24}$  dyne sec, as an estimate of a KT-sized impact. Synthetic displacement and strain records were generated for such a source by summing the normal modes of the elastic Earth model 1066A of Gilbert and Dziewonski [18]. We used the attenuation profile of the model PREM [19] to determine  $Q$  values for the 1066A modes. We assumed a vertically directed point source so we included only spheroidal modes in the synthetic seismogram

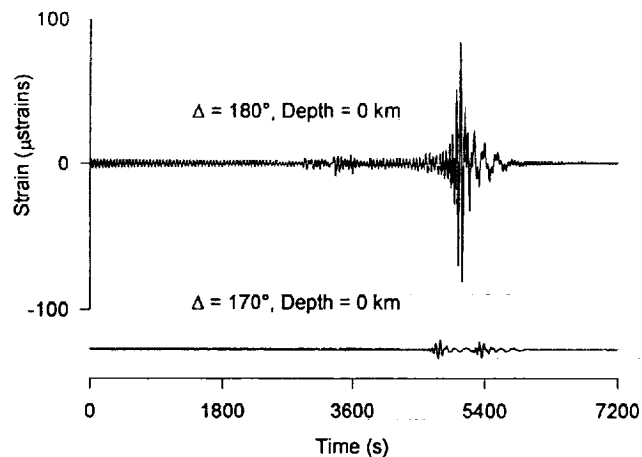


Fig. 1. Synthetic strain histories at and near impact antipode, plotted on same scale.

calculations. Toroidal modes are not excited by a vertical point force. All spheroidal modes with periods greater than 45 s were summed for the synthetics.

The synthetic signals yield estimates of the peak strains at any location in or on the Earth. Figure 1 shows the difference in strain histories on the Earth's surface at two different angular distances from the source. This figure demonstrates the gross effects of antipodal focusing. Strains at the surface near the antipode (angular distance =  $180^\circ$ ) are orders of magnitude higher than those over most of the rest of the Earth's surface. Figure 2 plots the peak strains as a function of depth beneath the antipode of the impact, from the surface to the core-mantle boundary. It can be seen that peak strain amplitude varies by 2 orders of magnitude and is largest at the top. This would imply that most of the energy is focused at shallow depths; however, it may be an artifact of ignoring shorter-period modes. This issue will be resolved by adding more modes, and by doing body wave calculations. Figure 3 demonstrates that focused arrivals have much greater amplitudes than direct arrivals at the core-mantle boundary. At the beginning of Fig. 3a, the direct arrival is shown for a point directly beneath the impact, followed by a long high-amplitude focused trace. For comparison, the strain history at the same level on the antipodal axis is shown in Fig. 3b. It can be seen to have a larger peak amplitude.

In addition to seismic modeling, we are in the process of performing detailed calculations of a hypothetical impact and subsequent wave propagation through the Earth with the CTH [20] strong-shock hydrodynamics code. CTH is a one-, two-, and three-dimensional multimaterial elastic-plastic Eulerian hydrodynamics code. CTH accurately computes the very large material deformations, material ejection, and strong-shock generation created by the initial KT impact. For these calculations we model the Earth as a central, gravitationally stable, stratified body, with a variety of interior structure, including inner and outer core and mantle. The materials are treated as elastic-plastic. Also, the equations of state associated

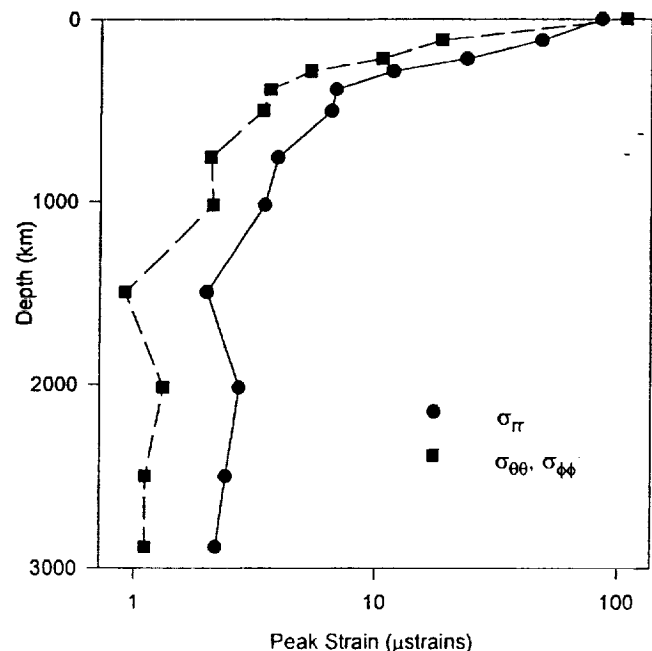
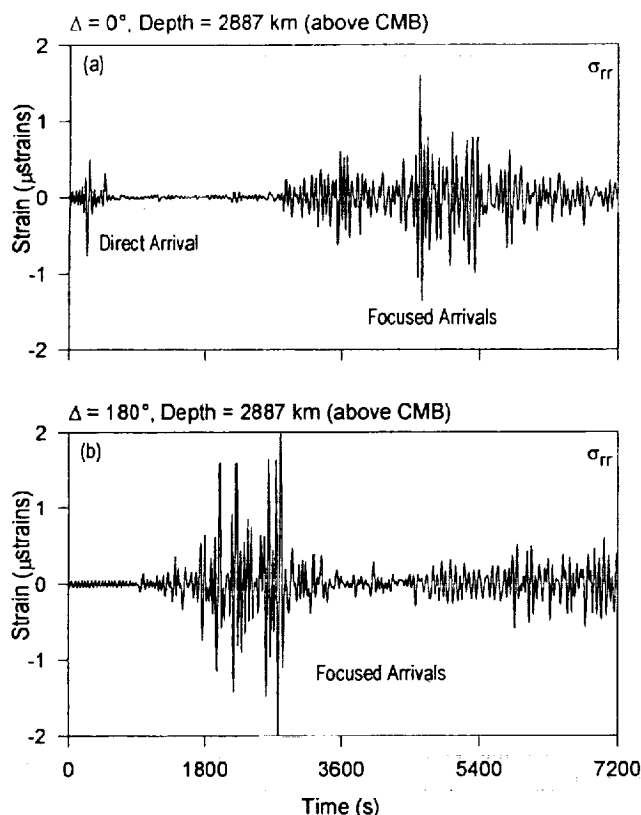


Fig. 2. Peak strain vs. depth along antipodal axis.



**Fig. 3.** Synthetic strain histories just above the core-mantle boundary (CMB) on the impact axis (a) beneath the impact and (b) antipodal to the impact.

with CTH allow thermodynamically consistent phase transitions, so that vaporization at the initial impact site can be properly modeled, as well as shock-wave modification in the Earth's interior due to solid-solid phase transitions. Alternatively, we have also modeled the initial impact site as a general energy source, similar in strategy to the seismic model and to the work of Watts et al. [10].

CTH can be used to study the long-term evolution of the resulting wave structures through the interior of the Earth, with some caveats related to accuracy. CTH is an artificial viscosity code, and numerically widens shock discontinuities. Generally speaking, at very long ranges and times the numerical dissipation in the code will cause inaccuracies in the almost linear wave propagation that is expected to occur. In particular, the numerical dissipation will attenuate stress waves at great propagation distances. In addition, resolution of these low amplitude waves as they propagate through regions of large hydrostatic compression in the Earth's interior must be maintained. While we have still studied the overall response of the antipodal region to the KT impact, the resulting amplitudes and strain due to the long-term wave interactions can be in error. Nonetheless, this approach has also been pursued by Watts et al. [10], and has led to useful investigation of the response of the antipodal region. Our numerical resolution is significantly finer than that of Watts et al. [10]. Ultimately, we will improve the accuracy of our numerical modeling by linking earlier time CTH results to the more accurate seismological analyses described earlier.

**Acknowledgments:** This work was performed at Sandia National Laboratories supported by the U.S. Department of Energy

under contract DE-AC04-76DP00789 with funding under the LDRD program.

**References:** [1] Seyfert C. K. and Sirkin L. A. (1979) *Earth History and Plate Tectonics*. [2] Burek P. J. and Wänke H. (1988) *Phys. Earth Planet. Inter.*, 50, 183–194. [3] Rampino M. R. and Strothers R. B. (1988) *Science*, 241, 663–668. [4] Glass B. P. et al. (1979) *Proc. LPSC 10th*, 25–37. [5] Pohl J. (1977) *Geol. Bavarica*, 75, 329–348. [6] Gutenberg B. and Richter C. (1934) *Gerlands Beitr. Geophys.*, 43, 56. [7] Rial J. A. (1979) Ph.D. Thesis, Caltech. [8] Chael (1983) Ph.D. Thesis, Caltech. [9] Schultz P. H. and Gault D. E. (1975) *Moon*, 12, 159–177. [10] Watts A. W. et al. (1991) *Icarus*, 93, 159–168. [11] Hagstrum J. T. and Turrin B. D. (1991) *Eos*, 72, 44, 516. [12] Rampino M. R. and Caldeira K. (1992) *GRL*, 19, 2011–2014. [13] Green D. H. (1972) *EPSL*, 15, 263–270. [14] Alt D. et al. (1988) *J. Geol.*, 96, 647–662. [15] Oberbeck V. R. et al. (1992) *J. Geol.*, 101, 1–19. [16] Negi J. G. et al. (1993) *Phys. Earth Planet. Inter.*, 76, 189–197. [17] Loper D. E. (1991) *Tectonophys.*, 187, 373–384. [18] Gilbert F. and Dziewonski A. M. (1975) *Phil. Trans. R. Soc. London*, A278, 187–269. [19] Dziewonski A. M. and Anderson D. L. (1981) *Phys. Earth Planet. Inter.*, 25, 297–356. [20] McGlaun J. M. et al. (1989) *Sandia National Laboratories Report SAND89-0607*.

omit to P.19

**TSUNAMI DEPOSITS AND THE KT BOUNDARY: A SEDIMENTOLOGIST'S PERSPECTIVE.** J. Bourgeois<sup>1,2</sup>, <sup>1</sup>Department of Geological Sciences, University of Washington, Seattle WA 98195, <sup>2</sup>Present address: at National Science Foundation, EAR Room 785, 4201 Wilson Boulevard, Arlington VA 22230, USA.

Tsunamis are impulse-generated waves and can be generated by any event that displaces a significant amount of water in a short period of time, on the scale of seconds to minutes. The most typical source of tsunamis are subduction zone earthquakes, when deformation associated with low-angle thrusting displaces water during the event. Tsunamis are also generated by volcanic events and subaqueous landslides; bolide impacts in water will produce the largest tsunamis in Earth history. Tsunamis are wave trains, rather than single waves, and they may be locally damped, focused, amplified, and reflected.

Our knowledge of typical (seismogenic) tsunamis and their deposits has increased significantly since Snowbird II. These tsunamis typically generate near field run-ups on the scale of meters, to tens of meters in rare cases. Recent tsunamis in Nicaragua (1992), Indonesia (1992), and Japan (1983, 1993) have allowed workers to generate detailed information about the nature of these tsunamis, their erosional and other destructive effects, and their deposits. Paleotsunami deposits from subduction-zone earthquakes have been documented from Chile (1960), Alaska (1964), the Pacific Northwest U.S. (late 1600s), and elsewhere. I will present a brief summary of the Nicaraguan, Chilean, and Pacific Northwest examples.

Tsunamis generated by bolide impacts ("megatsunamis") are at the other end of the tsunami scale, potentially generating tsunamis several orders of magnitude more energetic than seismogenic cases. Our understanding of these kinds of events is much more theoretical because there are no historic cases. We can expect that an impact in deep water could propagate a wave equal to the water depth, and thus megatsunamis may affect the floor of the ocean at depths much greater than seismogenic tsunamis, which only have an effect in the coastal zone. Certainly shelf environments (depths of ~30,200 m)